

Refractive-Index Profile Control Techniques in the Vapor-Phase Axial Deposition Method

Shoichi SUDO, Masao KAWACHI, Hiroyuki SUDA, Motohiro NAKAHARA and Takao EDAHIRO, *Regular Members*

UDC 681.7.068.2 : 535.326 : 666.192.091-911.3

SUMMARY A refractive-index profile formation mechanism in the VAD method for optical fiber preform fabrication was investigated and practical techniques for precisely controlling the preform index profile are proposed. The GeO_2 dopant distribution in the preform is found to be mainly caused by the porous VAD preform surface temperature distribution and by the raw material vapors mixing effect. By applying the surface temperature effect, the index profile can be controlled in the wide profile parameter range of $\alpha=1-10$. Further, by utilizing the mixing effect, it is possible to adjust the profile parameter precisely around a desired value. Transmission characteristics for graded-index fibers obtained with the above control technique are also presented.

1. Introduction

Since the development of the vapor-phase axial deposition (VAD) method in 1977⁽¹⁾, rapid progress has been made in VAD fabrication techniques. Especially, recent progress in the porous preform dehydration technique has led to producing a completely OH-free VAD fiber with lower OH-ion content than 1 ppb, which has lower loss than 1 dB/km in 1.1–1.7 μm wavelength range⁽²⁾. Graded-index fiber bandwidths has been also improved to a level of wider than 1 GHz.km⁽³⁾. Until now, however, refractive-index profile formation mechanism in the VAD process has not yet been fully clarified, because of the complicated flame hydrolysis reaction and deposition behavior.

In the early stage of the studies on the VAD process, the profile formation concept was determined on the basis that raw material vapors for different compositions, being blown out from different torch nozzles, mixed spatially with each other by diffusion and overlapped to form a spatial dopant distribution on the growing surface of the VAD porous preform^{(4), (5)}. This idea was ever thought to be dominant in the profile formation, but the experimental fact that graded-like profiles can be made even by use of a single torch with a single raw material vapor nozzle could not be explained by the above mixing effect idea only⁽⁶⁾.

Recent study on the $\text{SiO}_2\text{-GeO}_2$ particles deposition properties in the flame hydrolysis reaction has clarified

that the GeO_2 concentration in the deposited particles depends strongly on the substrate temperature during deposition, though the relation of these deposition properties to the practical fabrication conditions of graded-index VAD fibers has not yet been fully understood⁽⁷⁾.

The purpose of this paper is to clarify the detailed mechanism of the profile formation in the VAD process and to propose precise control techniques for graded-index profiles. Investigation emphasis is placed on clarifying both temperature effect and mixing effect, and on applying these effects to practical profile controlling. Transmission characteristics for graded-index fibers, fabricated using the proposed profile control techniques, are also presented.

2. Profile Formation Mechanism

2.1 Temperature Effect

The torch used for synthesizing fine glass particles by the flame hydrolysis reaction was composed of co-axial silica tubes, as illustrated in Fig. 1: nozzles I and II for halide material vapors and nozzle III for combustion gases of H_2 and O_2 .

Figure 2 illustrates the experimental arrangement used for investigating the temperature effect on the profile formation in the flame hydrolysis reaction⁽⁷⁾. In this experiment, a vapor-phase stream of $\text{SiCl}_4\text{-GeCl}_4$ (10 mol%) or $\text{SiCl}_4\text{-TiCl}_4$ (4 mol%) was blown out from nozzle I at a 165 cc/min rate, while no gas was blown out from nozzle II.

Fine glass particles synthesized in the flame were deposited onto a silica substrate tube (10 × 9 mm). The distance between the silica substrate tube and the torch end was 30 mm. The flame temperature was controlled by changing the H_2 and O_2 gas flow rates, and was measured

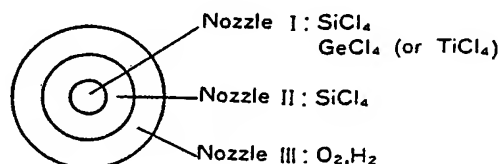


Fig. 1 Cross sectional structure of the torch used for synthesizing fine glass particles.

Manuscript received February 9, 1981.

Manuscript revised March 27, 1981.

The authors are with Ibaraki Electrical Communication Laboratory, N.T.T., Ibaraki, 319-11 Japan.
56-76 [P-58]

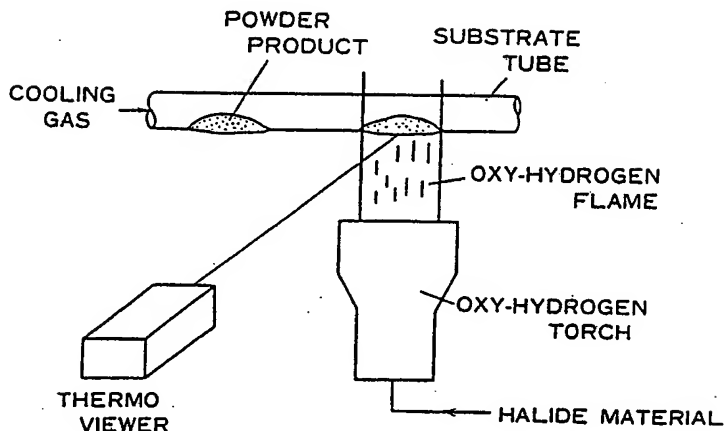


Fig. 2 Experimental arrangement used for investigating the temperature effect on the profile formation.

by inserting a thermocouple directly into the center part of the flame. The surface temperature of the substrate tube was maintained at a desired value by flowing cooling gas into the tube. The temperature was monitored using an optical pyrometer (JEOL, Thermo Viewer). Oxide particle product was deposited for 30 seconds for each deposition condition. The GeO_2 concentration in the deposited products was determined by the X-ray and IR measurement⁽⁷⁾.

Figure 3 shows a contour line map of the GeO_2 concentration in the $\text{SiO}_2\text{-GeO}_2$ system vs flame and substrate temperatures. Numerals represent the GeO_2 concentration in molar percent. It can be seen, in Fig. 3, that the GeO_2 concentration depends not only on substrate temperature but also on flame temperature. Under fixed flame temperature conditions of 1200°C and 1300°C, the GeO_2 concentration increases with increasing substrate temperature, while under a high fixed flame temperature condition of

1400°C, the GeO_2 concentration tends to decrease at higher substrate temperature than 700°C. The GeO_2 concentration decrease in the high flame and substrate temperature region in Fig. 3 might be attributed to the fact that the GeO_2 product is difficult to be deposited at a high temperature but it remains as a vapor state because of its high saturated vapor pressure in the flame⁽⁸⁾.

In the case of the $\text{SiO}_2\text{-TiO}_2$ system, neither the flame temperature dependence nor the substrate temperature dependence of the TiO_2 concentration was found. This is in sharp contrast to the case of the $\text{SiO}_2\text{-GeO}_2$ system; the reason could be sought in the difference in the saturated vapor pressure values between GeO_2 and TiO_2 ⁽⁷⁾.

The result in Fig. 3 indicates that care must be taken, both in regard to the flame and substrate temperatures during deposition for obtaining a desired profile in the case of the $\text{SiO}_2\text{-GeO}_2$ system.

2.2 Mixing Effect

Figure 4 is a drawing of the experimental apparatus used for investigating the raw material vapors mixing effect on index profile formation. The apparatus consists of a quasi-preform equipped with a hot gas heater, a glass synthesizing torch (Fig. 1) and a Thermo Viewer. The quasi-preform is similar in shape to the actual VAD porous preform growing end surface and is made of silica glass 50 mm in diameter and 0.3 mm thick.

A vapor-phase stream of $\text{SiCl}_4\text{-GeCl}_4$ (10 mol%) or $\text{SiCl}_4\text{-TiCl}_4$ (4 mol%) was blown from nozzle I into the flame at a rate of 165 cc/min and a pure SiCl_4 vapor stream was blown from nozzle II at a rate of 0–83 cc/min to induce the mixing effect between nozzle I and nozzle II. The quasi-preform surface temperature is controlled by varying the hot gas heater power in the temperature range from 500°C to 800°C, as measured at its maximum point.

Fine oxide particles synthesized by the flame hydro-

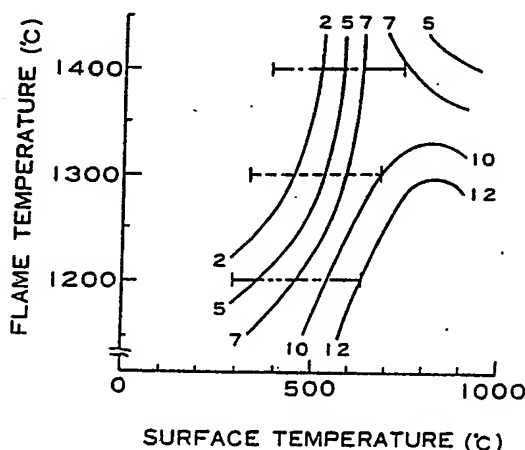


Fig. 3 Contour line map of the GeO_2 concentration in the $\text{SiO}_2\text{-GeO}_2$ system vs. the flame and substrate temperatures; numerals represent the GeO_2 concentration in molar percent.

lysis reaction were deposited on the quasi-preform surface to form a thin porous glass layer. Each deposition was continued for 1 minute to make an about 1 mm thick porous glass layer, as measured at the bottom surface of the quasi-preform.

Figures 5(a) and (b) show measured dopant concentration distribution on the quasi-preform for (a) $\text{SiO}_2\text{-GeO}_2$ system and (b) $\text{SiO}_2\text{-TiO}_2$ system. Curves A in Figs. 5(a) and (b) indicate dopant distributions obtained when (a) $\text{SiCl}_4\text{-GeCl}_4$ or (b) $\text{SiCl}_4\text{-TiCl}_4$ mixture was blown from nozzle I (165 cc/min) and no SiCl_4 vapor from nozzle II. Curves B represent the distribution formed when a SiCl_4 vapor (83 cc/min) was additionally blown from nozzle II.

The differences between curves A and curves B represent the mixing effect of raw materials blown from nozzle I and II.

Even when nozzle II is not used, a graded-like dopant distribution was obtained for the $\text{SiO}_2\text{-GeO}_2$ system (curve A in Fig. 5(a)). This may be attributed to the surface temperature distribution of the quasi-preform such that the temperature was high (650°C) at the center (bottom) part and decreased gradually to about 300°C along the radial direction of the quasi-preform surface. Then, the GeO_2 concentration at the surrounding part of the quasi-preform surface becomes about zero, in accordance with the result of Fig. 3. In the case of the $\text{SiO}_2\text{-TiO}_2$ system with nozzle II not used (curve A in Fig. 5(b)), almost step-like dopant distribution was formed as that expected from the experi-

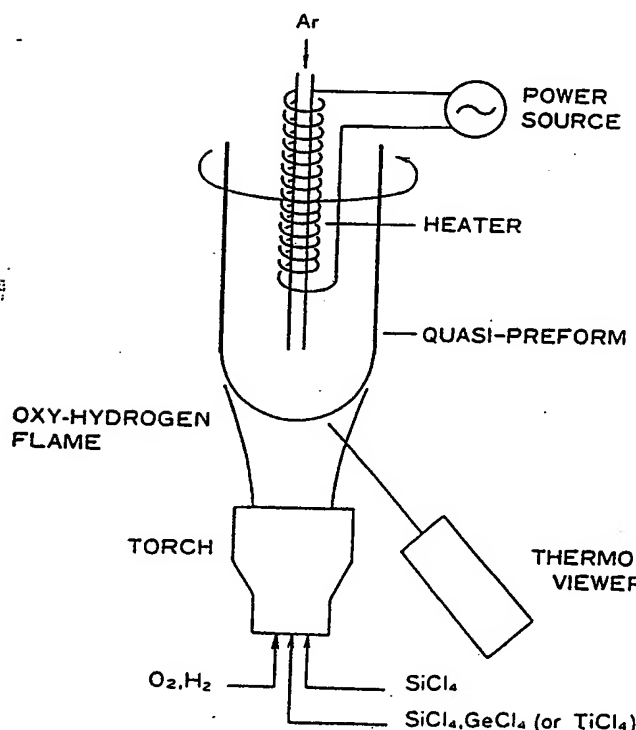


Fig. 4 Experimental apparatus used for investigating the raw material vapors mixing effect on the profile formation.

mental results of Sect. 2.1; a small deviation from the ideal step might be attributed rather to nonuniformity of the hydrolysis reaction in the radial direction of the flame.

The graded-like TiO_2 distribution in curve B in Fig. 5(b) is attributed largely to the mixing effect of the raw materials, while the graded-like GeO_2 distribution in curve B in Fig. 5(a) is caused by the superimposition of the temperature effect and the mixing effect.

The data for Fig. 5, being combined with the data for Fig. 3, offer useful guiding principles for precise control over the index profile in an actual VAD process. In the case of the $\text{SiO}_2\text{-GeO}_2$ system, both the flame temperature and the surface temperature distribution on the porous preform must be controlled suitably to make a desired

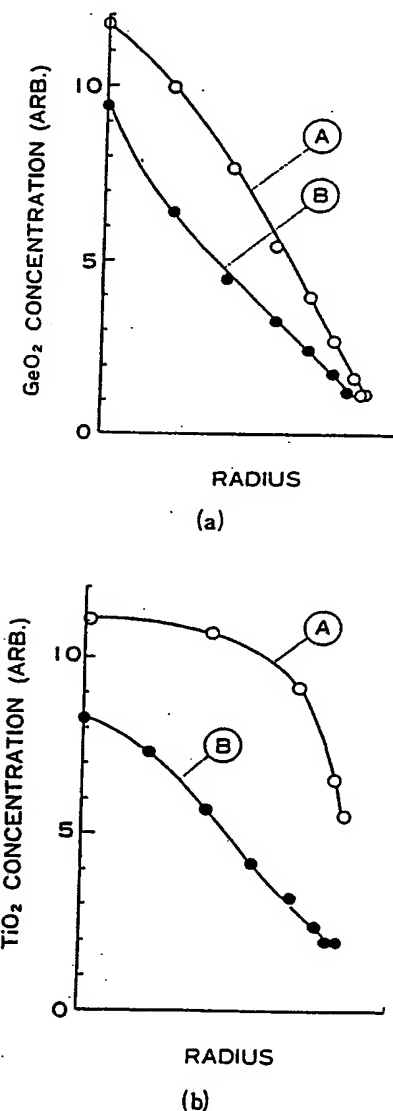


Fig. 5 Measured dopant concentration distribution on the quasi preform. (a) For the $\text{SiO}_2\text{-GeO}_2$ system. (b) For the $\text{SiO}_2\text{-TiO}_2$ system.

GeO_2 distribution profile; the mixing effect of the raw materials blown from multiple nozzles is also useful to modify the index profile. In the case of the $\text{SiO}_2\text{-TiO}_2$ system, the mixing effect of the raw materials is rather dominant in the profile formation, though low loss could not be expected in the $\text{SiO}_2\text{-TiO}_2$ glass fibers because of the partial appearance of Ti^{3+} ions in the glass. In the following, the glass composition is restricted to the $\text{SiO}_2\text{-GeO}_2$ system of practical importance.

3. Profile Control Technique

3.1 Experimental Procedures

The VAD apparatus used for graded-index fiber preform fabrication is shown in Fig. 6. A porous preform grown by the deposition of fine glass particles synthesized by the flame

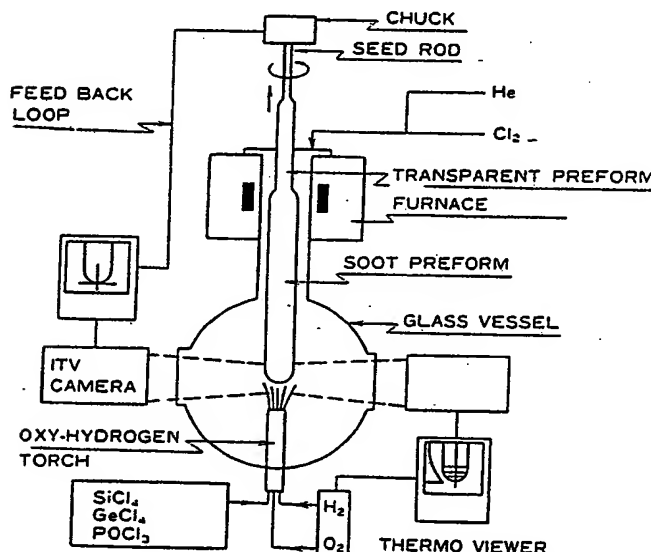


Fig. 6 VAD apparatus used for graded-index fiber preform fabrication.

hydrolysis reaction of SiCl_4 , GeCl_4 , POCl_3 is consolidated into a transparent preform by zone-melting in a carbon resistance furnace. A small amount of POCl_3 was added for deposition so as to decrease the sintering temperature of deposited porous preform, which eases consolidation at a relatively low temperature.

The growing end of the porous preform was controlled to be at a fixed position by the feed-back mechanism. Positional signal is obtained by the ITV camera system (Hamamatsu ITV C-1000), and the surface temperature distribution on the porous preform was measured using a Thermo Viewer.

A torch with the same structure as shown in Fig. 1 was applied for synthesizing fine glass particles. The porous preform was dehydrated in an atmosphere containing about 5 mol% Cl_2 gas simultaneously with consolidation in order to reduce the residual OH ions in the transparent preform. Transparent preform was elongated into an about 10 mm diameter rod, which was inserted into a silica tube to adjust the core/outer diameter ratio to the fiber specification.

The composited preform was then drawn into fibers 50 μm in core diameter and 125 μm in outer diameter. Parameters such as refractive index difference between core center and cladding, refractive index profile parameter and core diameter were evaluated by interference microscope measurement.

3.2 Surface Temperature Effect Application on Refractive Index Profile Control

On the basis of the profile formation mechanism investigation reported in Sect. 2, the surface temperature effect on the actual profile formation was studied; the surface temperature distribution on the porous preform end part was formed by regulating the hydrogen gas flow rate for combustion.

The mixture of SiCl_4 , GeCl_4 and POCl_3 vapors and the SiCl_4 vapor were blown out from nozzles I and II, respectively. A typical surface temperature distribution example is shown in Fig. 7. The temperature distribution

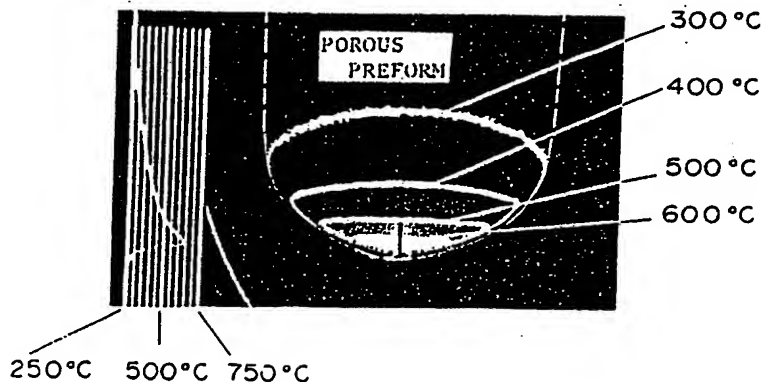


Fig. 7 Typical surface temperature distribution example for the porous preform growing end.

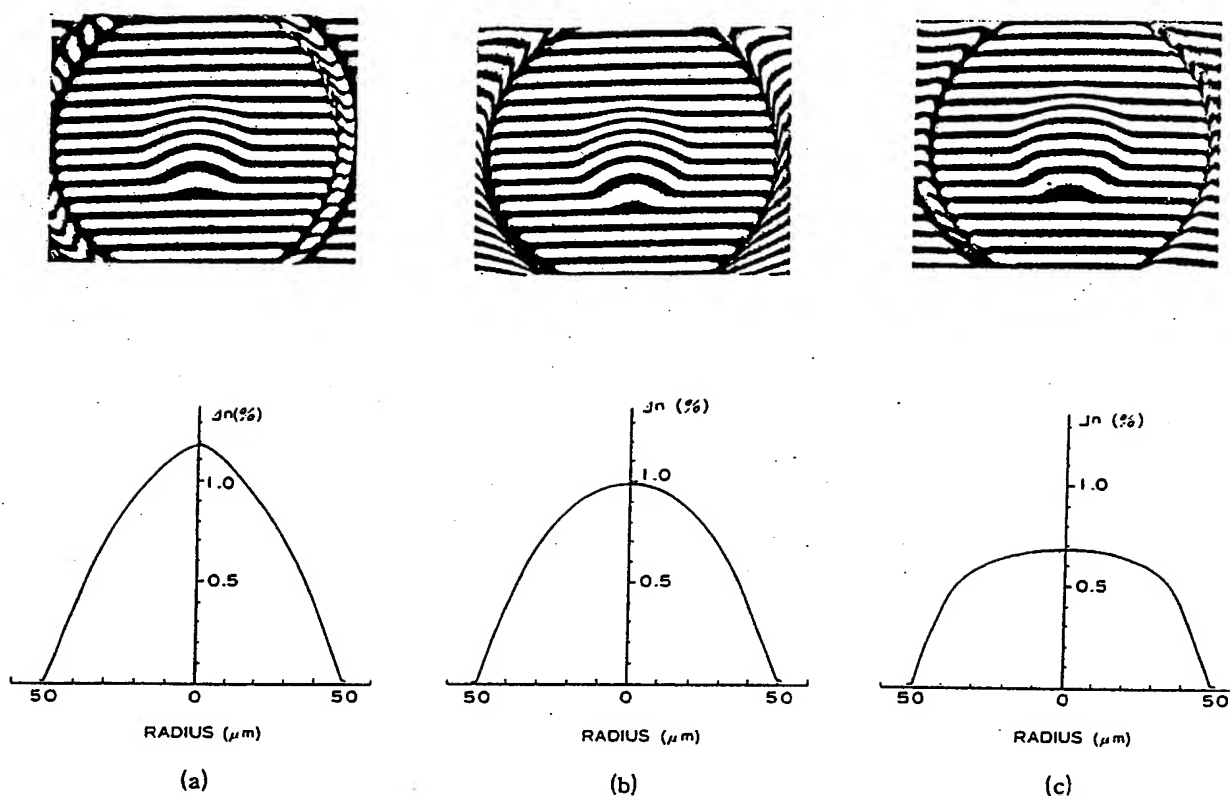


Fig. 8 Interference microscopic photographs and index profiles obtained under (a) 630°C, (b) 680°C and (c) 730°C maximum temperature.

along the center line of the preform is indicated on the left in Fig. 7, from which it can be seen that maximum temperature is about 650°C at the center part and the temperature decrease to 300°C gradually along the radial direction.

Interference microscopic photographs of fibers fabricated under (a) 630°C, (b) 680°C and (c) 730°C maximum temperature and (a) 1200°C, (b) 1300°C and (c) 1400°C flame temperature are shown in Fig. 8. Profile parameters for cases (a), (b) and (c) were 1.63, 1.95 and 3.94, respectively.

The profile parameter becomes larger according to increasing surface temperature, which is due to the substrate temperature dependence of the GeO_2 concentration. Figure 9 shows the relation between the maximum surface temperature and the profile parameter. The relation shown in Fig. 9 can be reasonably explained using the contour line map of the GeO_2 concentration. When the flame temperature is set at 1200°C and the surface temperature on the porous preform ranges from 630°C to 280°C, which is shown by two-dots-dash-line in Fig. 3, the GeO_2 concentration at the center part of the porous preform may become about 12 mol% and decrease gradually in the radial direction.

The GeO_2 concentration in the porous preform fabricated with 680°C maximum surface temperature and 1300°C

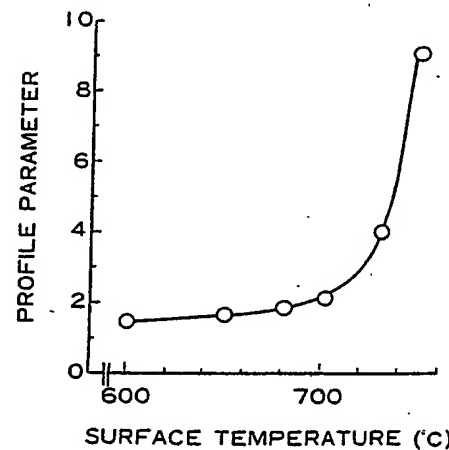


Fig. 9 Relation between maximum surface temperature and profile parameter.

flame temperature becomes about 10 mol% at the top and the refractive index profile becomes nearly parabolic (Fig. 8(b)), which can be deduced from the dash line data in Fig. 3.

When the flame temperature is elevated to 1400°C, the maximum GeO_2 concentration further decrease to about

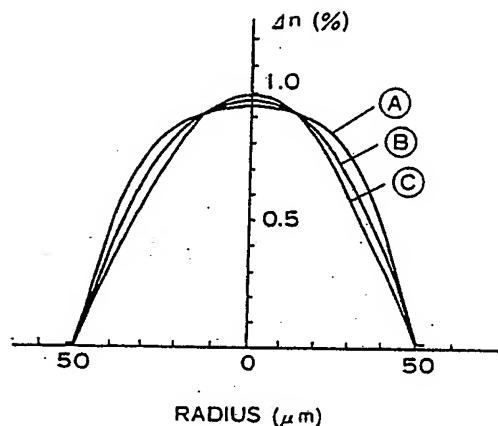


Fig. 10 Refractive-index profiles for fibers made under three flow rate ratio conditions of (A) $R=0.1$, (B) $R=0.3$ and (C) $R=0.5$.

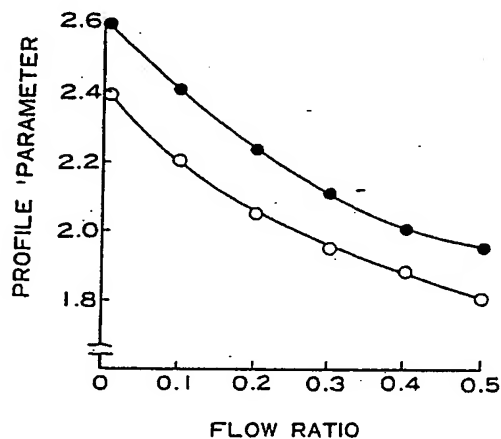


Fig. 11 Relation between material gas flow rate ratio and profile parameter.

7 mol% and the index profile becomes step-like (Fig. 8(c)), which can be understood from the dot-dash-line in Fig. 3.

The result shown in Fig. 9 suggests that the refractive index profile parameter can be controlled in a wide range of 1 to 10 by varying the porous preform surface temperature.

3.3 Mixing Effect Application on Refractive-Index Profile Control

As seen in the previous section, the refractive-index profile in the $\text{SiO}_2\text{-GeO}_2$ system is basically formed by the GeO_2 concentration substrate temperature dependence, but the precision of the profile determined by the temperature effect is rather rough, especially in the peripheral part. In the present section, mixing effect on the actual profile formation is investigated.

Flow rate ratio R for SiCl_4 vapor blown from nozzle II to $\text{SiCl}_4\text{-GeCl}_4\text{-POCl}_3$ vapor mixture from nozzle I was varied in three levels of (A) $R=0.1$, (B) $R=0.3$ and (C) $R=0.5$. Figure 10 shows refractive-index profiles for fibers made under the above three flow rate conditions. In each deposition condition, maximum temperature was kept at 650°C , which is the same value shown in Fig. 7. The profile parameter for each fiber was evaluated as 2.40 for fiber (A), 1.94 for fiber (B) and 1.83 for fiber (C).

Figure 11 shows the relation between the profile parameter and the material gas flow rate ratio. Solid circles and open circles in Fig. 11 indicate the profile parameters measured on the fibers fabricated under the maximum temperature conditions of 680°C and 650°C , respectively. It can be seen, from Fig. 11, that profile parameters decrease monotonically with increasing material gas flow rate ratio R . It can also be seen that the parameter at the fixed ratio shows a shift in the larger direction, according to the increase in the maximum temperature.

Figure 11 indicates that profile parameters for fibers

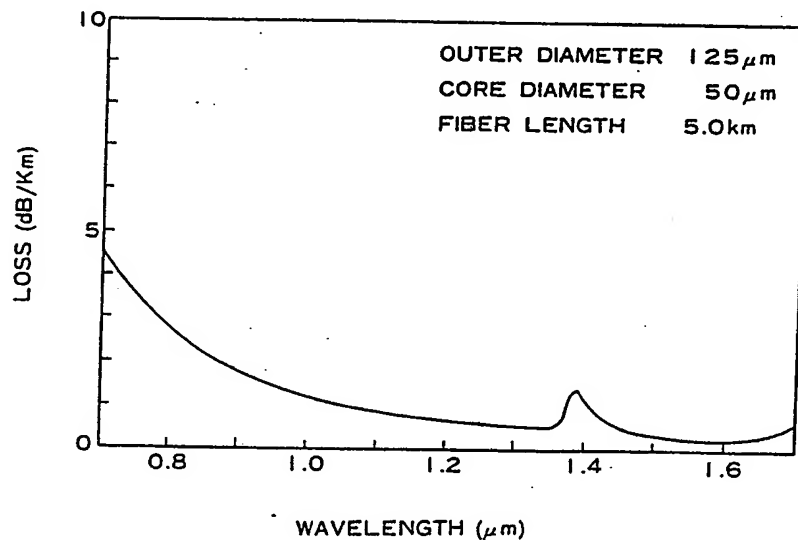


Fig. 12 Typical transmission loss spectrum for the graded-index fiber.

can be controlled to the desired value around 2.0, using the mixing effect on the profile formation along with the temperature effect.

4. Transmission Characteristics

Graded-index fibers, which are composed of a $\text{SiO}_2\text{-GeO}_2\text{-P}_2\text{O}_5$ core and a pure SiO_2 cladding, were fabricated by the above profile control technique. Figure 12 shows the typical transmission loss spectrum for the graded-index fibers, 5 km in length. Loss values at $1.3 \mu\text{m}$ and $1.6 \mu\text{m}$ wavelengths are 0.52 dB/km and 0.3 dB/km , respectively, and the residual OH-ion content is about 18 ppb.

Figure 13 shows the wavelength-dependence of 6-dB bandwidth measured for three 3 km fibers fabricated with the proposed profile control technique. The 6 dB bandwidths at 0.85 , 1.29 , 1.31 and $1.55 \mu\text{m}$ wavelengths were points measured with laser diodes. Plotted results are shown by solid circles. 6 dB bandwidths at the other wavelengths (open circles), ranging from 1.06 to $1.51 \mu\text{m}$, were measured with the fiber Raman laser. The experimental results shown in Fig. 13 indicate that optimum wavelengths of the three fibers are about $1.18 \mu\text{m}$, $1.31 \mu\text{m}$ and $1.51 \mu\text{m}$; 6 dB bandwidths at each optimum wavelength are $2.23 \text{ GHz}\cdot\text{km}^{0.9}$ ($\alpha=2.07$), $3.14 \text{ GHz}\cdot\text{km}^{0.9}$ ($\alpha=1.99$) and $2.15 \text{ GHz}\cdot\text{km}^{0.9}$ ($\alpha=1.94$), respectively.

Figure 14 shows the relation between the profile parameter and the 6 dB bandwidth at $1.3 \mu\text{m}$ wavelength. It is found from Fig. 14 that the 6 dB bandwidth wider than $1.0 \text{ GHz}\cdot\text{km}^{0.9}$ are obtained in the profile parameter range of 1.93 to 2.09 , and also that the optimum parameter at $1.3 \mu\text{m}$ wavelength is 1.99 ± 0.02 . This optimum parameter value is in good agreement with that evaluated experimentally in the MCVD fibers and also with the theoretical value reported in recent papers^{(9), (10)}.

5. Conclusion

Main results obtained in the present investigation on the refractive-index profile formation mechanism and its control technique in the VAD method are as follows:

- (1) In the $\text{SiO}_2\text{-GeO}_2$ system of practical importance, the GeO_2 concentration distribution in the preform is determined by the surface temperature distribution of the porous preform growing end and by the mixing effect between the raw material vapors.
- (2) Profile control technique has been proposed, where, by applying the temperature effect, the profile parameter can be controlled in the wide range of $\alpha=1\text{-}10$. By utilizing the mixing effect, the parameter can be adjusted precisely to the desired values around $\alpha=2.0$.
- (3) Graded-index VAD fibers, fabricated by the proposed profile control technique, exhibit good transmission properties. Bandwidth attained at the optimum wavelengths of $1.18 \mu\text{m}$, $1.31 \mu\text{m}$ and $1.55 \mu\text{m}$ are $2.23 \text{ GHz}\cdot\text{km}^{0.9}$, $3.14 \text{ GHz}\cdot\text{km}^{0.9}$ and $2.15 \text{ GHz}\cdot\text{km}^{0.9}$, respectively. The optimum profile parameter at $1.3 \mu\text{m}$ wavelength is ex-

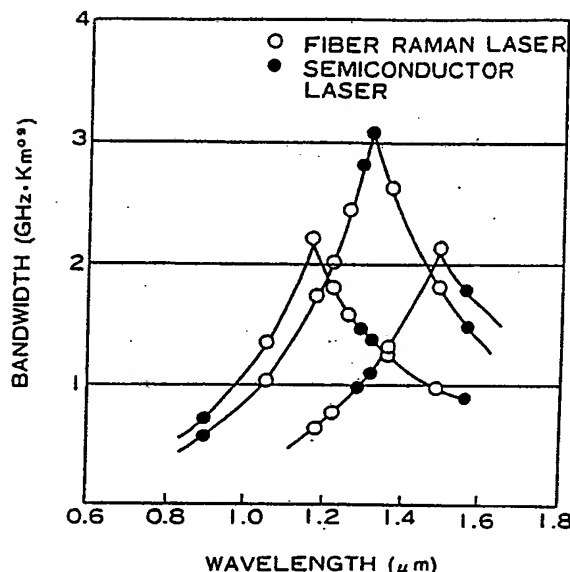


Fig. 13 Wavelength-dependence for 6 dB bandwidth measured for three 3 km graded-index fibers fabricated with the proposed profile control technique.

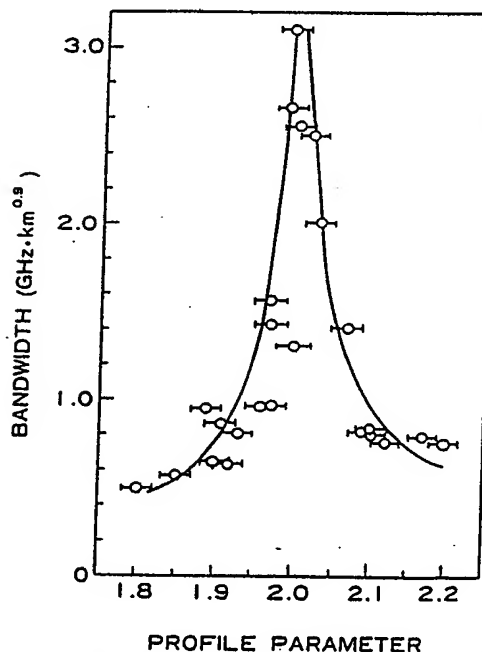


Fig. 14 Relation between profile parameter and bandwidth at $1.3 \mu\text{m}$ wavelength.

perimentally determined to be $\alpha=1.99 \pm 0.02$.

Acknowledgement

The authors would like to express their appreciations to N. Niizeki, H. Takata and N. Inagaki for their continuous encouragement and suggestions throughout the present study. They also indepted to T. Izawa, S. Takahashi, K. Chida and F. Hanawa for their helpful discussion and help.

Reference

- (1) Izawa, T., Kobayashi, S., Sudo, S. and Hanawa, F.: "Continuous fabrication for high silica fiber preform", 1977 International Conference on Integrated Optics and Communication Technical Digest, p. 375 (1977).
- (2) Hanawa, F., Sudo, S., Kawachi, M. and Nakahara, M.: "Fabrication of completely OH-free v.a.d. fiber", Electron. Lett., 16, 18, pp. 699-700 (1980).
- (3) Inagaki, N., Edahiro, T. and Nakahara, M.: "Recent progress in VAD fiber fabrication process", Digest of Technical Papers, the 12th Conference on Solid State Devices, B-1-2, pp. 25-26 (1980).
- (4) Izawa, T., Sudo, S. and Hanawa, F.: "Continuous fabrication process of high silica fiber preforms", Trans. IECE Japan, E62, 11, pp. 779-785 (Nov. 1979).
- (5) Yoshida, N., Tanaka, G., Kawahara, K., Sato, H., Kyoto, M., Hoshikawa, M., Okamoto, K. and Edahiro, T.: "Graded index profile formation and transmission characteristics of vad fiber", 6th European Conference on Optical Communication, p. 10 (1980).
- (6) Sanada, K., Shioda, T., Moriyama, T., Inada, K., Kawachi, M. and Takata, H.: "Refractive index profile control of the vapor phase axial deposition", Optical Communication Conference, conference proceeding, 5.1-1 (1980).
- (7) Edahiro, T., Kawachi, M., Sudo, S. and Tomaru, S.: "Deposition properties of high-silica particles in the flame hydrolysis reaction for optical fiber fabrication", Jpn. J. Appl. Phys., 19, 11, pp. 2047-2054 (1980).
- (8) Kawachi, M., Sudo, S. and Edahiro, T.: "Threshold gas flow rate of halide material for the formation of oxide particles in the VAD process for optical fiber fabrication", Jpn. J. Appl. Phys., 20, 4, pp. 709-712 (1981).
- (9) Kitayama, K., Seikai, S., Kato, Y., Uchida, N., Fukuda, O. and Inada, K.: "Transmission characteristics of long spliced graded-index optical fibers at $1.27 \mu\text{m}$ ", IEEE J. Quantum Electron, QE-15, 7, pp. 638-642 (1979).
- (10) Shibata, N. and Edahiro, T.: "Refractive-index dispersion of doped silica glasses for optical fibers", Paper of Technical Group, TGOQE80-114, IECE Japan (Dec. 1980).